Journal of Catalysis 257 (2008) 16–22

Contents lists available at ScienceDirect

Journal of Catalysis

www.elsevier.com/locate/jcat

Synthesis and characterization of γ-Al_2O_3-supported Pt catalysts from Pt_4 and Pt_6 clusters formed in aqueous solutions

Attilio Siani, Karen R. Wigal, Oleg S. Alexeev *, Michael D. Amiridis *

Department of Chemical Engineering, University of South Carolina, Columbia, SC 29208, USA

ARTICLE INFO

Article history:
Received 22 January 2008
Revised 27 March 2008
Accepted 27 March 2008
Available online 21 May 2008

Keywords:
Platinum clusters
PVA
EXAFS
CO adsorption
CO oxidation

ABSTRACT

Highly dispersed Pt catalysts were prepared by deposition of Pt_4 and Pt_6 clusters, initially formed in unprotected and poly(vinyl alcohol) (PVA)-protected colloidal Pt suspensions, onto a γ-Al_2O_3 surface. These catalysts were characterized by extended X-ray absorption fine structure (EXAFS) and Fourier transform infrared (FTIR) spectroscopies. The EXAFS results indicate that the supported Pt species formed were very similar in structure to those of the original clusters in the corresponding colloidal suspensions. The FTIR results further indicate that the γ-Al_2O_3-supported Pt_4 clusters have significantly lower chemisorptive properties compared with larger supported Pt nanoparticles; nevertheless, the Pt_4/γ-Al_2O_3 sample was active for the oxidation of CO with no need for additional activation treatment. In fact, treatment of this sample with H_2 at 150–200 °C led to the formation of Pt aggregates with sizes of 1.0–1.6 nm, demonstrating that the surface Pt_4 species readily sintered in this temperature range under reducing conditions.

1. Introduction

Conventional methods used for the preparation of supported metal catalysts involve the deposition of mostly inorganic metal precursors from solutions on the surfaces of metal oxide supports via incipient-wetness or wet-impregnation methods [1]. Subsequent decomposition of such precursors at elevated temperatures is needed to obtain catalytically active supported metal particles. In general, these conventional methods provide a very limited ability to control the structure of the resulting supported metal particles, and in many cases, the catalysts formed are nonuniform, with wide metal particle size distributions. In recent years, alternative synthetic routes based on the use of preformed clusters or templating agents (e.g., PAMAM dendrimers) have been proposed to obtain more uniform catalytic materials [2–5]. The primary focus in these preparation techniques is on precisely controlling the formation of metal bonds or metal particles in solution and then delivering them to the support surface in a way that preserves the morphology of the metal particles [6]. The application of such an approach remains problematic, however, at least in the case of Pt, because the removal of ligands or the templating agent leads to substantial Pt sintering [4,7].

We have previously demonstrated that stable and nearly uniform Pt_4 clusters can be formed in solution without the use of templating or protective agents [8]. Successful delivery of these Pt clusters to a support could potentially eliminate the need for further thermal treatments and thus decrease the likelihood of Pt sintering. To the best of our knowledge, no such attempts have been described in the literature to date, and the approach described in this paper represents the first time that γ-Al_2O_3-supported Pt catalysts have been prepared using an unprotected colloidal Pt suspension. The goal of this work was to evaluate how colloids of highly dispersed metal clusters can be used for the preparation of supported metal catalysts. We used UV–vis spectroscopy to investigate the deposition of Pt clusters from solution onto the γ-Al_2O_3 surface, and EXAFS and FTIR spectroscopies to characterize the surface species formed after the deposition of Pt onto the γ-Al_2O_3 surface. Finally, we evaluated the catalytic activity of the γ-Al_2O_3-supported Pt species for the gas-phase oxidation of CO.

2. Experimental

2.1. Reagents and materials

The γ-Al_2O_3 support (BASF), with a BET surface area of 100 m^2/g and a pore volume of 0.6 ml/g, was calcined in air at 500 °C for 4 h before use. H_2, He, and 1% CO/He (all UHP grade, Airstar) were purified before use via passage through oxygen/moisture traps (Agilent) capable of removing traces of O_2 to 15 ppb and traces of H_2O to 25 ppb. The 1% CO/air mixture (National Specialty Gases) was purified from traces of moisture via passage through a moisture trap (Agilent). $H_2PtCl_6{\cdot}6H_2O$ (99.95% purity, Alfa Aesar), sodium borohydride (98% purity, Alfa Aesar),

* Corresponding authors.
E-mail addresses: alexeev@engr.sc.edu (O.S. Alexeev), amiridis@engr.sc.edu (M.D. Amiridis).

0021-9517/$ – see front matter
doi:10.1016/j.jcat.2008.03.025

and low molecular weight polyvinyl alcohol (PVA) (Alfa Aesar) were used as supplied, while 18 MΩ cm Milli-Q deionized water was used for the preparation of all aqueous solutions.

2.2. Sample preparation

Unprotected and PVA-protected colloidal Pt suspensions were prepared as reported elsewhere [8]. Supported Pt/γ-Al_2O_3 samples were prepared by deposition of Pt from the unprotected colloidal solution onto the γ-Al_2O_3 surface. The γ-Al_2O_3 powder was added to the colloidal Pt solution, and the pH was decreased to approximately 2.0 with the addition of a 0.1 M hydrochloric acid solution. The resulting mixture was stirred vigorously for 30 min to allow complete deposition of Pt on the γ-Al_2O_3 surface. This process was monitored by UV–vis. After completion of the deposition step, any excess water was removed by filtration, the solid was washed with pure water until no chloride ions could be detected in the filtrate, and the resulting powder was dried under vacuum at room temperature. Additional Pt/γ-Al_2O_3 samples were prepared for comparison by a similar procedure using PVA-protected colloidal Pt suspensions. In both cases, a 0.4 wt% total Pt loading was chosen for the resulting Pt/γ-Al_2O_3 materials, confirmed by inductively coupled plasma-mass spectroscopy (ICP-MS) analysis (Galbraith Laboratories Inc.). The synthesis and handling of all Pt/γ-Al_2O_3 samples were carried out with standard air exclusion techniques using a Schlenk vacuum line and a N_2-filled dry box.

2.3. UV–vis spectroscopy

UV–vis spectra were obtained using a Shimadzu UV-2101PC spectrophotometer. The scan range was 800–190 nm, in 0.5-nm steps. Unless stated otherwise, 18 MΩ cm water (Milli-Q grade) was used as a reference for all measurements.

2.4. FTIR spectroscopy

FTIR spectra were collected with a Nicolet Nexus 470 spectrometer equipped with a MCTB detector cooled with liquid nitrogen. Powder samples were pressed into self-supported wafers with a density of 20 mg/cm^2 under approximately 5000 psi pressure and mounted in the FTIR cell connected to a gas distribution system. Each sample was pretreated *in situ* as described further in the text. When a reduction pretreatment was used, the temperature was ramped in H_2 at a rate of 5 °C/min to the desired value and then held there for 2 h. After the treatment was completed, the FTIR cell was flushed with He at the reduction temperature and then cooled to room temperature under He flow. FTIR spectra were recorded at a spectral resolution of 2 cm^{-1}, with 64 scans accumulated for each spectrum.

2.5. EXAFS spectroscopy

EXAFS spectra were collected at X-ray beamline 2–3 at the Stanford Synchrotron Radiation Laboratory (SSRL), Stanford Linear Accelerator Center, Menlo Park, CA. The storage ring electron energy was 3 GeV, and the ring current was in the range of 80–100 mA. The EXAFS data for Pt/γ-Al_2O_3 samples were recorded at room temperature in the fluorescence mode with a 13th element Ge detector. When a reduction pretreatment was used, the Pt/γ-Al_2O_3 powder samples were placed in a glass reactor and heated in H_2 as the temperature was ramped at 5 °C/min to the desired value and then maintained there for 2 h. Once the desired treatment was completed, the reactor was sealed and transferred into a dry box. Samples were loaded into *in situ* EXAFS fluorescence cells designed to allow handling of samples without air exposure. The total count rate for the Ge detector was 30,000–40,000 counts/s. It has been established experimentally that the detector readings are linear within this range, and that no corrections for dead-time are required. Samples were scanned at the Pt L_3 edge (11564 eV). Data were collected with a Si(220) double-crystal monochromator, which was detuned by 30% to minimize the effects of higher harmonics in the X-ray beam.

2.6. EXAFS data analysis

The EXAFS data were analyzed with experimentally determined reference files obtained from EXAFS data characterizing materials of known structure. The Pt–Pt and Pt–O interactions were analyzed with phase shifts and backscattering amplitudes obtained from EXAFS data characterizing platinum foil and $Na_2Pt(OH)_6$, respectively. The crystallographic first-shell coordination parameters for these reference compounds, the weighting of the Fourier transform, and the ranges in k and r space used to extract the reference functions from the experimental EXAFS data have been reported elsewhere [8]. The EXAFS parameters were extracted from the raw data using the XDAP software, developed by XAFS Services International [9]. The methods used to extract the EXAFS function from the raw data were essentially the same as reported elsewhere [10]. The data used for each sample were the averages of six scans.

The data at the Pt L_3 edge were analyzed with a maximum of 16 free parameters over the ranges $3.50 < k < 15.00$ Å^{-1} (where k is the wave vector) and $1.00 < r < 3.50$ Å (where r is the distance from the absorbing Pt atom). The statistically justified number of free parameters, n, was found to be 19, as estimated on the basis of the Nyquist theorem [11,12]: $n = (2\Delta k \Delta r/\pi) + 1$, where Δk and Δr are the k and r ranges used to fit the data. The parameters characterizing both the high-Z (Pt–Pt) and low-Z (Pt–O) contributions for the samples examined were determined by multiple-shell fitting in r-space with application of k^1 and k^3 weighting in the Fourier transformations [10]. The fit was optimized using a difference file technique with phase- and amplitude-corrected Fourier transformations of the data [13,14]. Some comparisons of the data and fits in r-space for a fresh Pt/γ-Al_2O_3 catalyst prepared from an unprotected colloidal Pt suspension are shown in Fig. 1, and the results for various supported samples are summarized in Table 1. The standard deviations reported in Table 1 for the various parameters were calculated from the covariance matrix, taking into account the statistical noise of the EXAFS data, as well as the correlations between the different coordination parameters, as described elsewhere [15]. Systematic errors were not included in calculation of the standard deviations. The goodness-of-fit values (ε_v^2) were calculated as outlined in the Reports on Standards and Criteria in XAFS Spectroscopy [16]. The variances in both the imaginary and absolute parts were used to determine the quality of the fit [17].

2.7. XANES measurements and analysis

XANES spectra of each sample were also obtained during the X-ray absorption measurements described above. Normalized XANES spectra were obtained by subtracting the pre-edge background from the raw data using a modified Victoreen equation, and dividing the absorption intensity by the height of the absorption edge. The band structure curves were numerically integrated using the XDAP software [5]. The observed band structure for the Pt L_3 edge, commonly called the "white line," is indicative of the absorption threshold resonances associated with the likelihood of excitation of $2p_{3/2}$ electrons to unoccupied d states [18]. It is generally assumed that the white line correlates with the electron density of metal atoms, with a decrease in the white line area indicating a decrease in the electron density of these atoms [18,19].

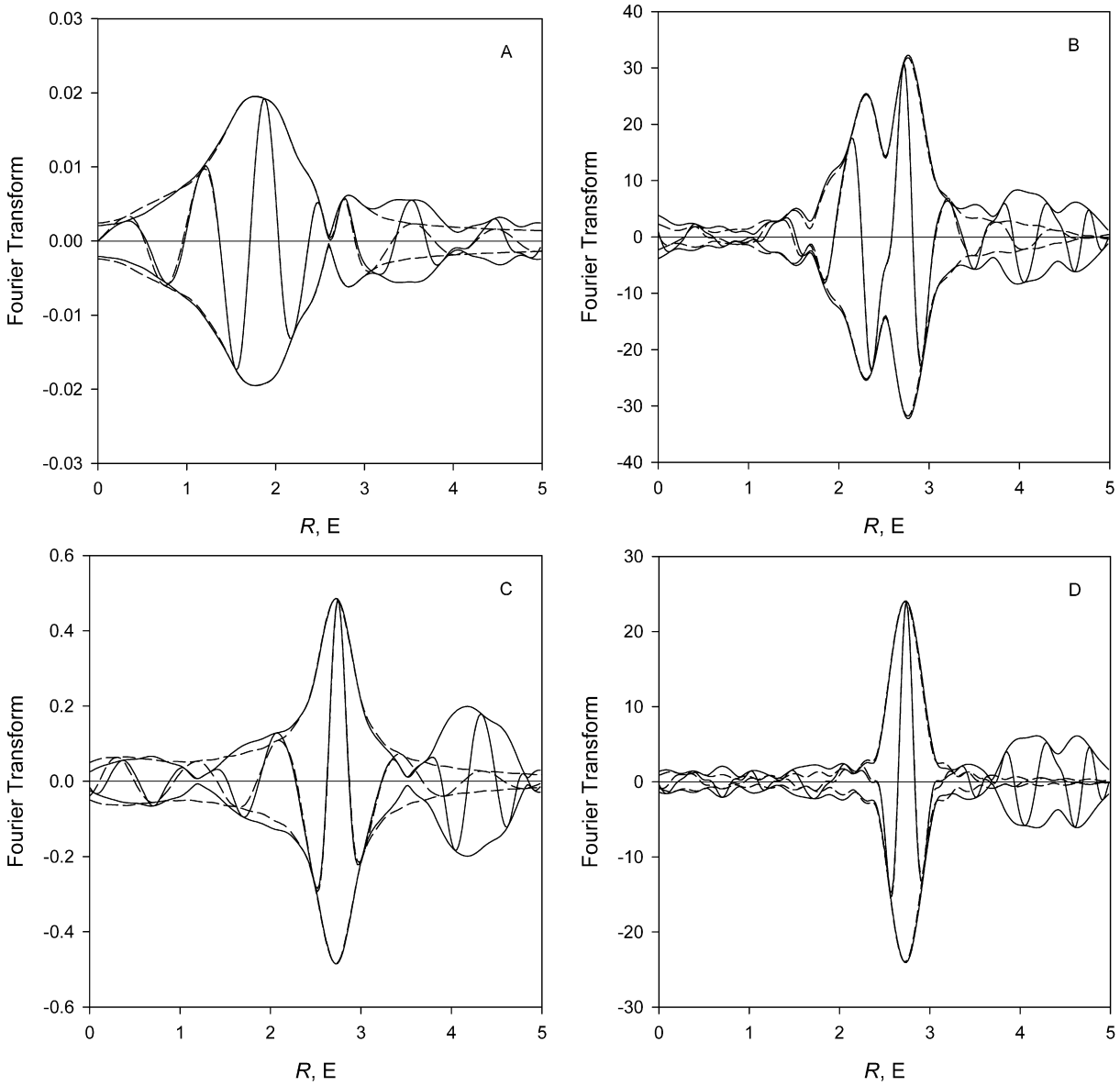

Fig. 1. EXAFS spectrum collected at the Pt L_3 edge and corresponding fits for a fresh Pt/γ-Al_2O_3 sample prepared from an unprotected colloidal Pt suspension: (A) imaginary part and magnitude of uncorrected Fourier transform (k^0-weighted, $\Delta k = 3.5$–15.0 Å^{-1}) of experimental EXAFS (solid line) and sum of the calculated contributions as stated in Table 1 (dashed line); (B) k^3-weighted Fourier transform of (A) plotted with Pt–Pt phase and amplitude correction; (C) and (D) residual spectra illustrating the Pt–Pt contributions: the imaginary part and magnitude of phase- and amplitude-corrected Fourier transforms (k^1 weighted (C) and k^3 weighted (D)) of the raw data minus Pt–O contributions (solid line) and the calculated first-shell Pt–Pt contributions (dashed line).

2.8. CO oxidation

Catalytic activity measurements for the oxidation of CO in air were performed in a quartz single-pass fixed-bed reactor at atmospheric pressure and temperatures of 25–300 °C. The temperature inside the reactor was monitored by a thermocouple extended into the catalyst bed. Samples in a powder form (0.077 g) were diluted 90 times by weight with quartz particles (60–80 mesh) to keep the catalyst bed isothermal. The total volumetric flow rate of the reactant mixture (1% CO balanced with air) was held at 154 ml/min (1 atm; 25 °C) yielding a corresponding gas hourly space velocity (GHSV) of approximately 120,000 ml/(g h). The feed and the reaction products were analyzed with an online single-beam NDIR CO analyzer (Ultramat 23, Siemens) capable of detecting CO in the 0–500 ppm and 0–5% ranges and CO_2 in the 0–5% range.

Catalytic measurements were performed with freshly prepared samples, as well as samples treated in H_2 at 150 and 200 °C. When a reduction pretreatment was conducted, the temperature was ramped in H_2 at 5 °C/min to the desired value and maintained there for 2 h. After the treatment was completed, the reactor was purged with N_2 at the reduction temperature and cooled to room temperature. The reaction mixture was introduced at that point, and data were collected at different times as the temperature was increased in 10–20 °C increments every 2 h. In the absence of a catalyst, no measurable conversion of CO was observed during background tests.

3. Results and discussion

3.1. Preparation of Pt/γ-Al_2O_3 catalysts from an unprotected Pt suspension

The impregnation of H_2PtCl_6 from aqueous solutions onto γ-Al_2O_3 has been extensively investigated [20–23]. Two major mech-

Table 1
Structural parameters characterizing Pt/γ-Al_2O_3 samples prepared from unprotected and PVA-protected colloidal Pt suspensions

Sample	Treatment conditions	Shell	N	R (Å)	$\Delta\sigma^2$ (Å^2)	ΔE_0 (eV)	ε_v^2	k^1-variances (%)		Suggested model of surface species
								Abs	Im	
Pt/Al_2O_3 prepared from an unprotected colloidal Pt suspension	None	Pt–Pt	2.8	2.75	0.00586	−6.0	3.3	2.5	4.1	Pt_4 clusters
		Pt–O_1	1.6	2.04	0.00210	−0.2				
		Pt–O_2	4.1	2.23	0.00790	−4.7				
		Pt–O_3	5.3	2.50	0.00880	4.3				
Pt/Al_2O_3 prepared from an unprotected colloidal Pt suspension	H_2 at 150 °C	Pt–Pt	6.1	2.74	0.00731	−4.8	3.3	2.6	3.4	Pt nanoparticles with average size of 1.0 nm
		Pt–O_1	2.0	2.05	0.01000	3.2				
		Pt–O_2	0.2	2.20	−0.00720	−5.0				
		Pt–O_3	0.4	2.53	−0.00701	2.0				
Pt/Al_2O_3 prepared from an unprotected colloidal Pt suspension	H_2 at 200 °C	Pt–Pt	7.9	2.74	0.00713	−6.4	3.6	2.1	4.7	Pt nanoparticles with average size of 1.6 nm
		Pt–O_1	0.8	2.02	0.01000	3.7				
		Pt–O_2	0.3	2.20	0.01000	4.2				
		Pt–O_3	0.6	2.53	−0.00066	−3.8				
Pt/Al_2O_3 prepared from a PVA-protected colloidal Pt suspension	None	Pt–Pt	4.0	2.74	0.00773	−5.1	3.2	2.2	3.4	Pt_6 clusters
		Pt–O_1	1.3	2.05	0.00120	−2.3				
		Pt–O_2	2.3	2.23	0.00090	−5.6				
		Pt–O_3	3.4	2.51	0.00570	2.7				

Note. N, coordination number; R, distance between absorber and backscatterer atoms; $\Delta\sigma^2$, difference in Debye–Waller factor between the sample and the reference compound; ΔE_0, inner potential correction accounting for the difference in the inner potential between the sample and the reference compound; ε_v^2, goodness of fit. Standard deviations in fits: $N \pm 20\%$, $R \pm 1\%$, $\Delta\sigma^2 \pm 5\%$, $\Delta E_0 \pm 10\%$.

anisms have been proposed to describe the attachment of this precursor to the surface. The first mechanism suggests that ligand exchange reactions occur between the anionic metal complex and the surface hydroxyl groups of γ-Al_2O_3 [22,23],

$$\text{Al–OH} + [\text{PtCl}_6]^{2-} \leftrightarrow \text{Al–}[(\text{OH})\text{PtCl}_5]^{-} + \text{Cl}^{-}, \quad (1)$$

whereas the second mechanism involves only electrostatic interactions between the metal complex and the charged hydroxyls on the Al_2O_3 surface [21],

$$\text{Al–OH}_2^{+} + [\text{PtCl}_6]^{2-} \leftrightarrow \text{Al–OH}_2^{+}\text{–}[\text{PtCl}_6]^{2-}. \quad (2)$$

The latter mechanism is based on experimental results indicating that the uptake of Pt by the support is increased as the pH of the impregnating solution is decreased. This effect has been attributed to an increase in the columbic attraction between the precursor and the support surface [21]. We have used this concept to develop a procedure that allows for the deposition of Pt_4 clusters from an aqueous solution onto the γ-Al_2O_3 surface.

As described previously, the high stability of the unprotected colloidal Pt suspension used can be attributed to the very low ionic strength of the solution and/or the electrostatic stabilization of the Pt_4 clusters formed, due to their interactions with ionic compounds present in the solution [6,8]. The Pt_4 clusters would be expected to be negatively charged under this scenario, although we have no experimental data to confirm such a claim. The behavior of such negatively charged Pt clusters in solution in the presence of the γ-Al_2O_3 support during pH changes would be somewhat similar to that of anionic Pt complexes. To test this hypothesis, γ-Al_2O_3 powder was added to a Pt_4 colloidal solution and the pH was lowered to approximately 2.0 with the addition of a 0.1 M hydrochloric acid solution. The resulting mixture was maintained under vigorous stirring, and the deposition process was monitored via UV–vis spectroscopy by filtering a portion of the solution at different times and analyzing the filtrate. The UV–vis band at 215 nm observed in the spectrum of the original solution and assigned previously to the isolated Pt_4 clusters [8,24], declined in intensity with time and finally disappeared after 30 min (Fig. 2). Atomic absorption analysis of the filtrate demonstrated a complete absence of Pt in the solution beyond that point, indicating that all of the Pt_4 clusters were deposited onto the γ-Al_2O_3 surface after approximately 30 min. It appears that such a deposition protocol was effective in the unprotected Pt_4 colloidal suspensions, reinforcing the idea that the Pt_4 clusters may be at least partially negatively charged in the original solution.

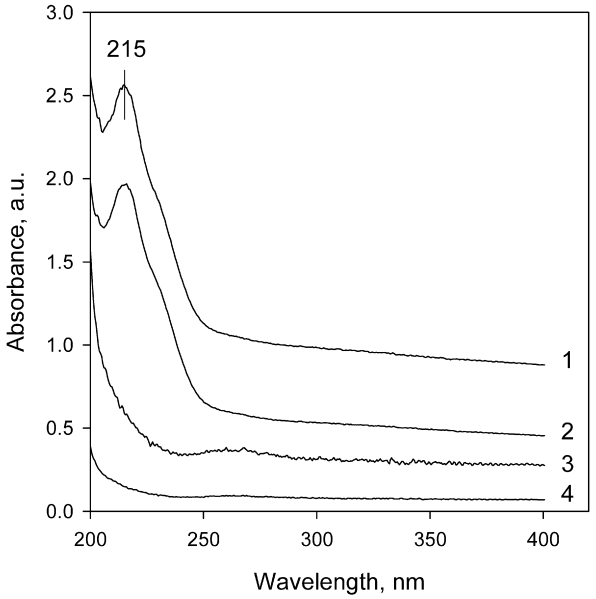

Fig. 2. UV–vis absorption spectra of aqueous solutions: (1) unprotected colloidal Pt suspension ($2.6 \cdot 10^{-4}$ M) and filtered solution following deposition of Pt onto γ-Al_2O_3 for (2) 10 min, (3) 20 min, and (4) 30 min.

The resulting Pt/γ-Al_2O_3 sample was dried under vacuum at room temperature and further characterized by EXAFS spectroscopy to probe the structure of the Pt surface species formed. The EXAFS results obtained with the freshly prepared sample (Table 1) indicate the presence of first-shell Pt–Pt contributions with an average coordination number of 2.8 at a bond distance of 2.75 Å. This distance is similar to that reported in the literature for larger γ-Al_2O_3-supported Pt clusters incorporating approximately 25 Pt atoms [25]. Moreover, the white line area characterizing this sample was nearly the same as that characterizing the corresponding Pt_4 clusters in solution (Table 2), indicating that platinum remained primarily in a reduced state after impregnation on the support. The low Pt–Pt coordination number, combined with the fact that no higher Pt–Pt shells were observed in the spectra, suggest that Pt remained highly dispersed on the γ-Al_2O_3 surface in

Table 2
XANES data for various Pt samples in solution and on a γ-Al_2O_3 support

Experiment	Sample	White line area	Reference
S1	H_2PtCl_6/H_2O treated with $NaBH_4$ at 25 °C	4.3	[8]
S2	H_2PtCl_6/H_2O treated with $NaBH_4$ at 25 °C in the presence of PVA	4.6	[8]
S3	Pt/γ-Al_2O_3 prepared from (S1)	4.7	This work
S4	S3 treated with H_2 at 150 °C	4.5	This work
S5	S3 treated with H_2 at 200 °C	4.3	This work
S6	Pt/γ-Al_2O_3 prepared from (S2)	4.8	This work

the form of isolated and nearly uniform Pt clusters consisting of approximately four Pt atoms.

In addition to the Pt–Pt contributions, substantial Pt–O contributions were also observed in the spectra at average distances of 2.04, 2.23, and 2.50 Å (Table 1). None of these contributions directly matched known Pt–O contributions for various platinum oxides (i.e., Pt_3O_4, PtO_2, and PtO), suggesting that no such species were formed on the alumina surface after the deposition of Pt. Instead, the observed Pt–O contributions appear to represent the interactions of the Pt clusters with the support. Such a conclusion is consistent with previous reports indicating that Pt–$O_{support}$ contributions with average distances in the range of 2.05–2.29 and 2.50–2.80 Å are typical for Pt supported on various metal oxides [2]. The nature of the Pt–$O_{support}$ contributions observed in the 2.50–2.80 Å range has been extensively discussed in the literature [26–28]. In contrast, the presence of two Pt–$O_{support}$ contributions in the first coordination shell of Pt at average distances of 2.04 and 2.20 Å is rather unusual for Pt/γ-Al_2O_3 catalysts. It is possible that these contributions represent interactions of Pt with both the oxygen atoms of the support and oxygen-containing species present on the catalyst surface, because evacuation at room temperature did not completely remove water from γ-Al_2O_3. Furthermore, the coordination number for the Pt–O contributions at approximately 2.20 Å decreased significantly after subsequent treatment with H_2 at elevated temperatures (Table 1), indicating that this contribution is the most temperature-dependent. Consequently, one possible explanation is that this contribution represents interactions of Pt atoms with water molecules present on the catalyst surface and located in close proximity to the Pt_4 clusters.

In summary, the foregoing results demonstrate that our synthetic approach allows the deposition of intact Pt_4 clusters preformed in an aqueous solution onto the surface of a γ-Al_2O_3 support. More importantly, these results provide the first evidence that highly dispersed and nearly uniform Pt_4 clusters can be formed on the γ-Al_2O_3 surface without the use of surfactants or templating agents.

3.2. Preparation of Pt/γ-Al_2O_3 catalysts from a PVA-protected Pt suspension

PVA-protected Pt_6 clusters formed in aqueous solution [8] were also delivered onto γ-Al_2O_3 by adding the γ-Al_2O_3 support to the solution under stirring at a pH of 2.0. After 30 min of adsorption time, the slurry was filtered and the sample was washed with water until the filtrate was free of Cl^- ions. Finally, the sample was dried under vacuum at room temperature and analyzed by EXAFS spectroscopy. The results of the EXAFS data analysis reported in Table 1 indicate the presence of Pt–Pt contributions with an average coordination number of 4.0 at a bonding distance of 2.74 Å, as well multiple Pt–$O_{support}$ contributions with average coordination numbers of 1.3, 2.3, and 3.4 at corresponding bonding distances of 2.05, 2.23, and 2.51 Å. These Pt–$O_{support}$ contributions are the same as those observed for the sample prepared from the unprotected colloidal Pt suspension reported in the previous section. In the PVA-protected suspension, however, some of the Pt-(Low-Z) backscatterers may also represent the PVA macromolecules that were not removed. The structural parameters characterizing the Pt–Pt contributions in the Pt/γ-Al_2O_3 material (Table 1) are nearly the same as those characterizing the Pt_6 clusters in the PVA-protected solution [8], suggesting that the Pt_6 clusters were delivered intact onto the γ-Al_2O_3 surface in this case as well. Moreover, analysis of the XANES region indicates once again that the white line area did not change substantially after the impregnation procedure (Table 2), implying that the Pt_6 clusters remained primarily in a reduced state on the γ-Al_2O_3 surface.

Small clusters have been prepared on various supports in the case of Ru, Ir, and Rh [2,29–31], but not yet for Pt, which is widely used as a catalyst in large-scale industrial and environmental applications [32]. Previous reports indicate that attempts to synthesize supported Pt carbonyl clusters have been successful only in the case of basic MgO, with $[Pt_6(CO)_{12}]^{2-}$, $[Pt_9(CO)_{18}]^{2-}$, and $[Pt_{15}(CO)_{30}]^{2-}$ species formed [33,34]; however, successful decarbonylation with no loss of nuclearity has been reported only for $[Pt_{15}(CO)_{30}]^{2-}$/MgO [33,34]. In all other cases, Pt metallic aggregates of various sizes were formed even under moderate decarbonylation conditions [33,34]. In this regard, the data reported in this paper demonstrate for the first time that the immobilization of both unprotected and PVA-protected colloidal Pt suspensions on γ-Al_2O_3 represent synthetic routes for preparing highly dispersed and nearly uniform supported Pt catalysts with the same morphology of the Pt species as in the colloidal suspensions used as precursors.

3.3. Sintering during H_2 treatments

Pt/γ-Al_2O_3 samples prepared from unprotected colloidal Pt suspensions were subsequently treated in H_2 at elevated temperatures and characterized by EXAFS spectroscopy to determine the structure of the surface species formed. When the H_2 treatment was conducted at 150 °C, first-shell Pt–Pt contributions with an average coordination number of 6.1 at a bonding distance of 2.74 Å were observed in the spectra (Table 1). When the treatment temperature was increased to 200 °C, the first-shell Pt–Pt coordination number was further increased to 7.9, indicating that the Pt_4 clusters initially present on the γ-Al_2O_3 surface underwent substantial sintering under these conditions. All Pt–O contributions initially observed and attributed to the interactions of the Pt clusters with the support became less significant with increasing temperature of the H_2 treatment, supporting the idea of Pt sintering. The dimensions of the Pt surface species formed can be estimated from the EXAFS data based on models correlating the average metal particle size to the first-shell metal–metal coordination number [35,36]. It was previously shown that such estimates are in good agreement with those obtained from hydrogen chemisorption measurements and HRTEM [37,38]. The EXAFS data indicate that the H_2 treatment at 150 and 200 °C led to the formation of Pt nanoparticles with average sizes of approximately 1.0 and 1.6 nm, respectively. Assuming that these particles have a spherical shape, these sizes correspond to platinum dispersions (i.e., fraction of metal atoms exposed) of approximately 100% and 69%, respectively.

3.4. CO adsorption

The FTIR spectrum collected at room temperature following exposure of a fresh Pt/γ-Al_2O_3 sample prepared from the unprotected Pt suspension to a 1% CO/He mixture is shown in Fig. 3 (spectrum 1). This spectrum consists of a single band centered at 2068 cm^{-1}, which can be assigned to terminal CO species adsorbed on fully reduced Pt sites [39]. The absence of any bands

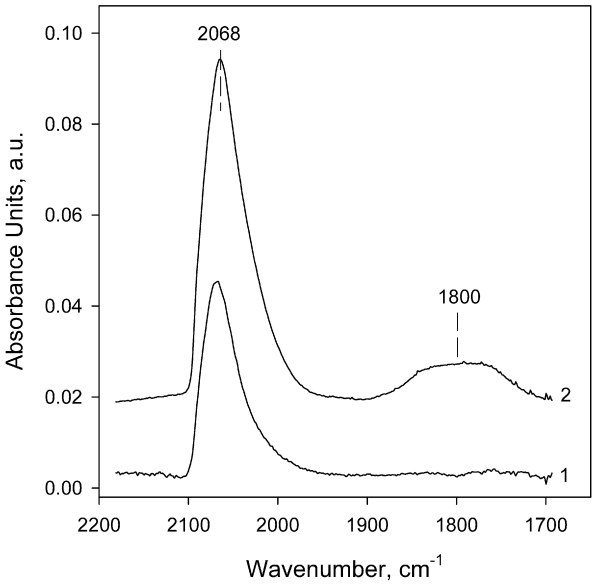

Fig. 3. FTIR spectra of CO adsorbed at room temperature on the Pt/γ-Al_2O_3 sample prepared from an unprotected colloidal Pt suspension: (1) as prepared and (2) following H_2 treatment at 200 °C.

corresponding to bridging CO species in the 1700–1900 cm^{-1} region of the spectrum indicates the presence of Pt in a highly dispersed form on the γ-Al_2O_3 surface, consistent with the EXAFS data suggesting the presence of Pt_4 clusters. These Pt_4 clusters remained isolated on the γ-Al_2O_3 surface and (given the limited number of Pt atoms per cluster) restricted the formation of bridge-bonded CO species. Therefore, the FTIR data support the EXAFS and XANES data reported above, and confirm that the Pt_4 clusters initially formed in the unprotected colloidal suspension were delivered onto the γ-Al_2O_3 surface with no significant changes in their electronic or structural properties.

When the Pt/γ-Al_2O_3 catalyst was further treated in H_2 at 200 °C before being exposed to the 1% CO/He mixture at room temperature, the band of the terminal CO species centered at 2068 cm^{-1} increased in intensity (Fig. 3, spectrum 2). A second broad band also appeared in the spectrum at approximately 1800 cm^{-1}, indicating the presence of bridging CO species [39]. This latter feature suggests that sintering of Pt occurred under these treatment conditions, in agreement with the EXAFS results, which also suggest that the H_2 treatment at 200 °C led to the formation of Pt nanoparticles with an average particle size of approximately 1.6 nm.

The spectra shown in Fig. 3 indicate that the freshly prepared sample, containing primarily Pt_4 species, chemisorbed approximately 2.4-fold less CO than the sample treated in H_2 at 200 °C. Because the dispersion of Pt in the freshly prepared sample was nearly 100%, this result suggests that the supported Pt_4 clusters had significantly lower chemisorptive properties compared with the larger supported Pt nanoparticles. It was previously shown that the chemisorption of both H_2 and CO on MgO- and γ-Al_2O_3-supported iridium species strongly depends on the cluster or aggregate size [40–42]; more specifically, a sharp increase in the H/Ir and CO/Ir values was observed when the average size of the Ir clusters or aggregates was increased from 6 Å to 12 Å [40–42]. The reason for this behavior is not clear; however, it has been suggested that when supported metal clusters incorporate only a few metal atoms, the support affects the reactivity of such clusters to an extent similar to that for a multidentate ligand [43].

3.5. CO oxidation in air

In Pt/γ-Al_2O_3 catalysts prepared from polymer-protected Pt suspensions, the catalytically active metal sites are shielded by the polymer from access by potential reactants, and thus a polymer removal step is needed to make such samples catalytically active [44,45]. Therefore, for the Pt/γ-Al_2O_3 catalysts prepared from the PVA-protected Pt suspensions, a procedure for PVA decomposition and removal that minimizes any significant changes in the structure of the supported Pt_6 clusters is needed. This task is beyond the scope of the present work. In contrast, no such procedure is needed (at least in principle) for the Pt/γ-Al_2O_3 materials prepared from the unprotected colloidal Pt suspensions. Thus, the oxidation of CO in air was used as a test reaction to determine whether these materials indeed exhibit any significant catalytic activity without the need for additional treatment. Fig. 4 shows the CO conversions recorded at various reaction temperatures, along

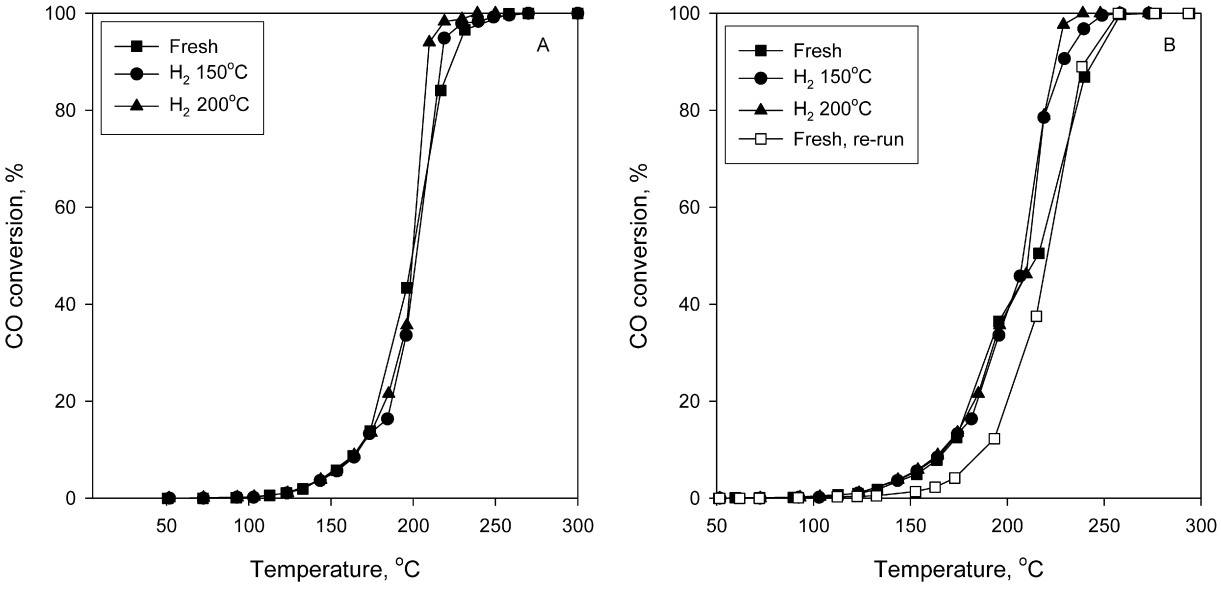

Fig. 4. CO conversions observed at different temperatures under CO oxidation conditions for Pt/γ-Al_2O_3 catalysts prepared from an unprotected colloidal Pt suspension: (A) initial and (B) steady-state conversions for a freshly prepared sample (□, ■), as well as samples treated in H_2 at 150 (●) and 200 °C (▲). (Reaction conditions: 1% CO, balance air, space velocity 120,000 ml/(g h).)

with the catalytic behavior of samples subsequently treated in H_2 at 150 and 200 °C for comparison. Both initial and "steady-state" (i.e., after 2 h on stream) conversions were measured at each temperature; these are reported in Figs. 4A and 4B, respectively. The freshly prepared sample exhibited CO conversions similar to those of the samples treated in H_2 at 150 and 200 °C in the 50–200 °C temperature range in which CO conversions remained <50%, indicating that CO oxidation proceeded at approximately the same rate over Pt_4 clusters and Pt nanoparticles ranging in size from 1 to 1.6 nm. With further increases in reaction temperature, some small differences were observed among the samples; for example, although a comparison of the light-off curves collected under initial and steady-state conditions (Figs. 4A and 4B) indicates that some deactivation occurred in all cases, this deactivation was more pronounced for the fresh sample. Furthermore, this sample was less active than the H_2-treated samples at temperatures above 210 °C, and complete conversion of CO was observed only at approximately 260 °C. We previously reported that γ-Al_2O_3-supported Pt particles can undergo structural changes under CO oxidation conditions [38]. Such changes were attributed to high surface coverage of Pt by oxygen at high CO conversion, inducing partial disintegration of the Pt particles and leading to the formation of Pt oxide-like species, which are less active for CO oxidation [38]. The highly dispersed and nearly uniform Pt_4 clusters present in the fresh sample would be expected to be the most susceptible to such structural changes. Retesting of the fresh Pt/γ-Al_2O_3 catalyst used for the CO oxidation measurements with no additional treatment between tests yielded a light-off curve exhibiting substantially lower activity at temperatures of 50–230 °C (Fig. 4B) and activity similar to that of the original sample at temperatures above 230 °C. Such a behavior indeed is consistent with the occurrence of some restructuring during exposure to reaction conditions at higher temperatures, leading to the unusual shape of the light-off curve observed for the fresh sample. Nevertheless, the CO oxidation results demonstrate that γ-Al_2O_3-supported Pt_4 clusters prepared from the unprotected colloidal Pt suspension were active for the oxidation of CO with no additional activation. Moreover, the structure of these clusters and thus their activity in this reaction could be altered in the presence of reactants at elevated temperatures.

4. Conclusion

Unprotected and PVA-protected colloidal Pt suspensions containing nearly uniform Pt_4 and Pt_6 clusters, respectively, can be used as precursors for the preparation of supported Pt catalysts. Our EXAFS findings indicate that the Pt_4 and Pt_6 clusters initially formed in solution can be delivered nearly intact onto a γ-Al_2O_3 support. Pt_4/γ-Al_2O_3 samples prepared from the unprotected colloidal Pt suspension were found to be active for the oxidation of CO in air with no need for additional activation treatment; however, the structure of the highly dispersed γ-Al_2O_3-supported Pt_4 clusters obtained can be substantially altered under CO oxidation conditions at elevated temperatures.

Acknowledgments

This work was supported by the U.S. Department of Energy, Office of Basic Energy Sciences (DE-FG02-05ER15731 and DE-FG02-05ER14980). A part of this research was carried out at the Stanford Synchrotron Radiation Laboratory (SSRL), a national user facility operated by Stanford University on behalf of the U.S. Department of Energy, Office of Basic Energy Sciences. The authors thank the beam line staff at SSRL for their assistance. The EXAFS data were analyzed using the XDAP software, developed by XAFS Services International [9].

References

[1] G. Ertl, H. Knözinger, J. Weitkamp (Eds.), Preparation of Solid Catalysts, Wiley, Weinheim, 1999.
[2] O.S. Alexeev, B.C. Gates, Top. Catal. 10 (2000) 273.
[3] M. Zhao, L. Sun, R.M. Crooks, J. Am. Chem. Soc. 120 (1998) 4877.
[4] O.S. Alexeev, A. Siani, G. Lafaye, C.T. Williams, H.J. Ploehn, M.D. Amiridis, J. Phys. Chem. B 110 (2006) 24903.
[5] A. Siani, O.S. Alexeev, D.S. Deutsch, J. Monnier, P.T. Fanson, H. Hirata, S. Matsumoto, C.T. Williams, M.D. Amiridis, manuscript in preparation.
[6] A. Roucoux, J. Schulz, H. Patin, Chem. Rev. 102 (2002) 3757.
[7] B.C. Gates, Chem. Rev. 95 (1995) 511.
[8] A. Siani, K.R. Wigal, O.S. Alexeev, M.D. Amiridis, J. Catal. 257 (2008) 5.
[9] M. Vaarkamp, J.C. Linders, D.C. Koningsberger, Physica B 208–209 (1995) 159.
[10] D.C. Koningsberger, in: C.A. Melendres, A. Tadjeddine (Eds.), Synchrotron Techniques in Interfacial Electrochemistry, Kluwer, Dordrecht, 1994, p. 181.
[11] E.A. Stern, Phys. Rev. B 48 (1993) 9825.
[12] E.O. Brigham, The Fast Fourier Transform, Prentice–Hall, Englewood Cliffs, NJ, 1974.
[13] P.S. Kirlin, F.B.M. van Zon, D.C. Koningsberger, B.C. Gates, J. Phys. Chem. 94 (1990) 8439.
[14] J.B.A.D. van Zon, D.C. Koningsberger, H.F.J. van't Blik, D.E. Sayers, J. Chem. Phys. 82 (1985) 5742.
[15] M. Vaarkamp, Ph.D. thesis, Eindhoven University, The Netherlands, 1993.
[16] F.W. Lytle, D.E. Sayers, E.A. Stern, Physica B 158 (1988) 701.
[17] D.C. Koningsberger, B.L. Mojet, G.E. van Dorssen, D.E. Ramaker, Top. Catal. 10 (2000) 143.
[18] J.H. Sinfelt, in: Y. Iwasawa (Ed.), X-ray Absorption Fine Structure for Catalysts and Surfaces, World Scientific Publishing, Singapore, 1996.
[19] J.H. Sinfelt, G.D. Meitzner, Acc. Chem. Res. 26 (1993) 1.
[20] W.A. Spieker, J. Liu, J.T. Miller, J. Kropf, J.R. Regalbuto, Appl. Catal. A Gen. 232 (2002) 219.
[21] W.A. Spieker, J. Liu, J.T. Miller, J. Kropf, J.R. Regalbuto, Appl. Catal. A 243 (2003) 53.
[22] J.P. Boitiaux, J.M. Deves, B. Didillon, C.R. Marcilly, in: G.J. Antos, A.M. Aitani, J.M. Parera (Eds.), Catalytic Naphtha Reforming, Science and Technology, Marcel Dekker, New York, 1995, p. 79.
[23] J.H.A. Martens, R. Prins, Appl. Catal. 46 (1989) 31.
[24] C. Burda, X. Chen, R. Narayanan, M.A. El-Sayed, Chem. Rev. 105 (2005) 1025.
[25] O.S. Alexeev, F. Li, M.D. Amiridis, B.C. Gates, J. Phys. Chem. B 109 (2005) 2338.
[26] M. Vaarkamp, F.S. Modica, J.T. Miller, D.C. Koningsberger, J. Catal. 144 (1993) 611.
[27] S.E. Deutsch, G. Mestl, H. Knözinger, B.C. Gates, J. Phys. Chem. B 101 (1997) 1374.
[28] A.M. Ferrari, K.M. Neyman, M. Mayer, M. Staufer, B.C. Gates, N. Rösch, J. Phys. Chem. B 103 (1999) 5311.
[29] K. Asakura, Y. Iwasawa, J. Chem. Soc., Faraday Trans. 86 (1990) 2657.
[30] O. Alexeev, G. Panjabi, B.C. Gates, J. Catal. 173 (1998) 196.
[31] W.A. Weber, B.C. Gates, J. Phys. Chem. B 101 (1997) 10423.
[32] R.J. Farrauto, C.H. Bartholomew, Fundamentals of Industrial Catalytic Processes, Wiley, Chichester, 2003.
[33] J. Puga, R. Patrini, K.M. Sanchez, B.C. Gates, Inorg. Chem. 30 (1991) 2479.
[34] S.K. Purnell, K.M. Sanchez, R. Patrini, J.R. Chang, B.C. Gates, J. Phys. Chem. 98 (1994) 1205.
[35] B.J. Kip, F.B.M. Duivenvoorden, D.C. Koningsberger, R. Prins, J. Catal. 105 (1987) 26.
[36] R.B. Greegor, F.W. Lytle, J. Catal. 63 (1980) 476.
[37] E.S. Shpiro, R.W. Joyner, K.M. Minachev, P.D.A. Pudney, J. Catal. 127 (1991) 366.
[38] O.S. Alexeev, S.Y. Chin, M.H. Engelhard, L. Ortiz-Soto, M.D. Amiridis, J. Phys. Chem. B 109 (2005) 23430.
[39] L.H. Lyttle, Infrared Spectra of Adsorbed Species, Academic Press, London, UK, 1975.
[40] O.S. Alexeev, D.-W. Kim, B.C. Gates, J. Mol. Catal. A 162 (2000) 67.
[41] F.-S. Xiao, Z. Xu, O.S. Alexeev, B.C. Gates, J. Phys. Chem. 99 (1995) 1548.
[42] O.S. Alexeev, G. Panjabi, B.C. Gates, J. Catal. 173 (1998) 196.
[43] Z. Xu, F.-S. Xiao, S.K. Purnell, O. Alexeev, S. Kawi, S.E. Deutsch, B.C. Gates, Nature 372 (1994) 346.
[44] D.S. Deutsch, G. Lafaye, D. Liu, B.D. Chandler, C.T. Williams, M.D. Amiridis, Catal. Lett. 97 (2004) 139.
[45] D.S. Deutsch, A. Siani, P.T. Fanson, H. Hirata, S. Matsumoto, C.T. Williams, M.D. Amiridis, J. Phys. Chem. C 111 (2007) 4246.